



Heat transfer for falling film evaporation of black liquor up to very high Prandtl numbers [☆]



Erik Karlsson ^{a,*}, Mathias Gourdon ^a, Lars Olausson ^b, Lennart Vamling ^a

^a Energy and Environment, Chalmers University of Technology, Gothenburg, Sweden

^b Metso Power AB, Gothenburg, Sweden

ARTICLE INFO

Article history:

Received 21 January 2013

Received in revised form 2 July 2013

Accepted 3 July 2013

Available online 30 July 2013

Keywords:

Heat transfer

Falling film

Evaporation

High Prandtl numbers

High viscosity

Black liquor

ABSTRACT

In this study, heat transfer measurements for falling film evaporation were performed up to very high Prandtl numbers, from 10 to 2800. Black liquor, a residual stream from the pulping process, was used as an example of a fluid that can have very high Prandtl numbers. To overcome the problem with fouling, which can be severe for black liquor due to crystal formation at higher concentrations, a new measurement method has been successfully developed which enables reliable measurements. Viscosity was clearly the most important parameter for the heat transfer coefficient, while the specific mass flow rate had a weak and positive dependence. The results were compared with existing heat transfer correlations, but none of them were able to capture the heat transfer behavior of black liquor throughout the whole range of Prandtl numbers.

© 2013 The Authors. Published by Elsevier Ltd. All rights reserved.

1. Introduction

Falling film evaporation is a robust technology used in various industrial applications. In particular it is a proven technology for fluids with high Prandtl numbers (and viscosity), which for example is the case for highly concentrated milk in milk powder production and so called black liquor in the pulp and paper industry. The aim of this paper was to experimentally investigate evaporating falling film heat transfer for black liquor, as an example of a fluid that can have very high Prandtl numbers, and to investigate how existing correlations, developed for lower Prandtl numbers, agree with the experimental results.

The black liquor evaporation plant is an essential part of a chemical pulp mill. Black liquor, which is a residual stream from the pulping process, needs to be recycled for both environmental and economic reasons. In the liquor recovery cycle, black liquor is concentrated in a multi-stage evaporation plant before being combusted in a recovery boiler. The evaporation plant is the largest consumer of steam at the mill and thus good understanding of heat transfer properties is important. Black liquor is inherently known

for having high viscosity and to cause significant problems with fouling.

Black liquor is a complex viscous alkaline solution of water and organic and inorganic components, where the composition varies from pulp mill to pulp mill due to different cooking conditions and wood properties. One of the most important properties of black liquor is the dry solids mass fraction (or dry matter content, here denoted S) since it is a measure of the total concentration of non-aqueous components. In industrial multiple effect evaporators, the black liquor is normally concentrated from about 0.15 to 0.75 dry solids mass fraction, some even up to 0.85, using about 5–7 effects.

The physical properties of black liquor change significantly when it is concentrated, and the strong increase of viscosity is one of the most important changes. At low dry solids mass fraction the rheological properties are close to water, but at about 0.5 dry solids mass fraction the liquor is gradually transformed from a polymer solution to a polymer-continuous phase resulting in a more rapid increase of viscosity. At increased temperature the viscosity decreases, and this is used to prevent the viscosity of becoming too high as the concentration increases in the evaporator effects [1]. The Prandtl number is a function of specific heat (c_p), dynamic viscosity (μ) and thermal conductivity (k), but viscosity show a much higher dependency of dry solids mass fraction and temperature compare to the others and therefore the Prandtl number follows the viscosity.

[☆] This is an open-access article distributed under the terms of the Creative Commons Attribution-NonCommercial-ShareAlike License, which permits non-commercial use, distribution, and reproduction in any medium, provided the original author and source are credited.

* Corresponding author. Tel.: +46 31 772 3015.

E-mail address: erik.karlsson@chalmers.se (E. Karlsson).

Nomenclature

A	area (m ²)
c_p	specific heat (W/m ² K)
g	gravitational acceleration (m/s ²)
h	heat transfer coefficient (W/m ² K)
K	constant
k	thermal conductivity (W/m K)
P	parameter
Q	rate of heating (W)
q	heat flux (W/m ²)
S	dry solids mass fraction (kg/kg)
T	temperature (K)
U	overall heat transfer coefficient (W/m ² K)
δ	thickness (m)
μ	dynamic viscosity (Pa s)
ν	kinematic viscosity (m ² /s)
ρ	density (kg/m ³)
Γ	liquid flow rate per a unit width (kg/m s)
σ	surface tension (N/m)

Ka	Kapitza number
Nu	Nusselt number
Pr	Prandtl number
Re	Reynolds number

Subscripts

bl	black liquor
i	inside
lam	laminar flow
m	mean value
o	outside
steam	heating steam
trans	laminar–turbulent transition
tot	total value
turb	turbulent flow
w	evaporator tube wall

At about 0.5 dry solids mass fraction, sodium salts starts to precipitate and form crystal particles in the liquor. Depending on liquor composition, these particles contributes to about 10% of the mass at $S = 0.8$ and have a maximum size of about 100 μm . However, the crystallization will also occur on the heat transfer surface leading to fouling, and can in some situations be rapid and severe. This will complicate measurements of the heat transfer coefficient and is one reason why previous work on black liquor falling film heat transfer has mainly focused on low to intermediate dry solids mass fractions ($0.25 < S < 0.55$) [2–5]. In the present work, a new experimental procedure had to be developed to enable accurate measurements of heat transfer at high dry solids fractions for black liquor, which imply very high viscosities and thus very high Prandtl numbers.

In contrast to the experimental or empirical approach used in this study, numerical simulations of the flow characteristics and heat transfer of the falling film can be done. However, this approach faces many difficulties; mainly because of the complexity in capturing the evolution of the free liquid surface and also due to the large difference in the scale of the dimensions (length versus film thickness). Chen and Gao [6] simulated black liquor falling film evaporation based on elliptic incompressible Navier–Stokes equations in 2D. However, their results were not verified and did not include wave hydrodynamics. Doro [7] used Direct Numerical Simulation (DNS) of Navier–Stokes equations and was able to model black liquor falling film evaporation with converged results in 2D, but only for relatively low flow rates.

2. Models for falling film free surface evaporation

Dimensionless numbers are often used for modeling and general characterization of heat transfer, where the heat transfer coefficient, h , is described by the Nusselt number. For falling film free surface evaporation the standard definition of the Nusselt number is [8]:

$$Nu \equiv \frac{h}{k} \left(\frac{\nu^2}{g} \right)^{1/3}, \quad (1)$$

where k is the thermal conductivity, ν the kinematic viscosity and g the gravitational acceleration.

To model the heat transfer a correlation is normally used where the Nusselt number is a function of Prandtl, Reynolds and/or other dimensionless numbers. The general correlations available for heat transfer in falling film evaporation have primarily been developed for fluids with relatively low Prandtl numbers, and the majority of them are based on experimental data for Prandtl numbers below 7. Their range of validity is in most cases also limited to a certain flow regime (laminar, wavy-laminar or turbulent flow), characterized by the Reynolds number. Different definitions of the Reynolds number are found in the literature, and here the following is used:

$$Re \equiv \frac{4\Gamma}{\mu}, \quad (2)$$

where Γ is the mass flow rate per unit width, hereinafter called specific mass flow rate.

The general heat transfer correlations normally have one expression for laminar flow and one for turbulent flow. The transition from laminar flow with capillary or roll waves to the turbulent flow regime is suggested by Chun and Seban [9] to be Prandtl number dependent according to the following expression:

$$Re_{\text{trans}} = 5800Pr^{-1.06}. \quad (3)$$

Previous work on black liquor at low to intermediate solids mass fractions (< 0.55) [10] has shown that none of the available models in literature give good agreement with measured experimental data. For Prandtl numbers above 52, extrapolation of correlations by Chun and Seban [9] and Schnabel and Schlünder [8] lead to values that are closest to the experimental results. Chun and Seban [9] proposed the following model for the heat transfer during falling film evaporation:

$$Nu_{\text{lam}} = 0.822Re^{-0.22}, \quad (4)$$

$$Nu_{\text{turb}} = 0.0038Re^{0.4}Pr^{0.65}. \quad (5)$$

However, the model was based on a limited set of Prandtl values between 1.77 and 5.7.

Schnabel and Schlünder [8] based their model on a review of measurements from different authors for a limited number of fluids and a small interval of Prandtl numbers between 1.75 and 7, and proposed the following model:

$$Nu_{\text{lam}} = 1.43Re^{-1/3}, \quad (6)$$

$$Nu_{\text{turb}} = 0.0036Re^{0.4}Pr^{0.65}. \quad (7)$$

In the transition region between laminar and turbulent flow they suggested a superposition by the power of two, which will give a more gradual transition compared to Chun and Seban [9]:

$$Nu = (Nu_{\text{lam}}^2 + Nu_{\text{turb}}^2)^{1/2}. \quad (8)$$

In a recent work by Arndt and Scholl [11], the heat transfer was measured at higher Prandtl numbers, up to 155, and for a range of Reynolds numbers between 52 and 3760 based on experiments using cyclohexanol and propylene glycol. They concluded that none of the available literature models are reliable for high Prandtl numbers. For cyclohexanol they developed the following model:

$$Nu_{\text{lam}} = 0.57 \left(\frac{Re}{4} \right)^{-0.08}, \quad (9)$$

$$Nu_{\text{turb}} = 0.84 Nu_{\text{turb, Alhusseini}}, \quad (10)$$

where $Nu_{\text{turb, Alh}}$ is the turbulent Nusselt number from Alhusseini [12]:

$$Nu_{\text{turb, Alh}} = \frac{Pr \delta^{+1/3}}{(A_1 Pr^{3/4} + A_2 Pr^{1/2} A_3 Pr^{1/4} + C_1) + (B Ka^{1/2} Pr^{1/2})} \quad (11)$$

with

$$A_1 = 9.17,$$

$$A_2 = \frac{0.328\pi(130 + \delta^+)}{\delta^+},$$

$$A_3 = \frac{0.0289(152100 + 2340\delta^+ + 7\delta^{+2})}{\delta^{+2}},$$

$$B = \frac{2.51 \cdot 10^6 \delta^{+1/3} Ka^{-0.173}}{Re^{3.49} Ka^{0.0675}},$$

$$C_1 = 8.82 + 0.0003Re,$$

$$\delta^+ = 0.0946Re^{0.8},$$

and the Kapitza number defined as:

$$Ka \equiv \frac{g\mu^4}{\rho\sigma^3}. \quad (12)$$

Arndt and Scholl used the following superposition in the transition region between laminar and turbulent flow:

$$Nu = (Nu_{\text{lam}}^5 + Nu_{\text{turb}}^5)^{1/5}. \quad (13)$$

For propylene this model, however, did not predict their experimental data well, rather they saw a significant over-prediction from the model. Their conclusion was that a significantly broader data base was required.

Johansson et al. [2] also developed a new correlation, but solely for black liquor. This correlation was based on experimental data in the region of $4.7 < Pr < 170$ and $47 < Re < 6740$, and dry solids mass fractions up to 0.51. It was based on the correlation by Schnabel and Schlünder [8] but added a dry solids mass fraction dependence, and also included a Reynolds number limit for where the Nusselt numbers ceased to increase, described by the following equations:

$$Nu_{\text{lam}} = 1.43Pr^{-1/3}, \quad (14)$$

$$Nu_{\text{turb}} = 0.0036[\min(Re_{\text{exp}}, Re_{\text{limit}})]^{(0.4-0.125S)} Pr^{0.65}, \quad (15)$$

$$Nu = (Nu_{\text{lam}}^2 + Nu_{\text{turb}}^2)^{1/2}, \quad (16)$$

where S is the dry solids mass fraction and Re_{limit} is given by:

$$Re_{\text{limit}} = 13500Pr^{-0.85}. \quad (17)$$

The Reynolds number limit for stagnant heat transfer should not be confused with the transitional Reynolds number, which describes at what Reynolds number there is a transition from laminar to the tur-

bulent flow regime. The limit in Reynolds number for this correlation was introduced as the general formulation over-predicted the experimental results. Two tentative explanations were given; one is that the liquid in the large waves in the falling film behaves as isolated lumps undergoing recirculation, and the other is sputtering at high specific mass flow rates. The dependence on the dry solids fraction in the turbulent part of the correlation suppresses the increase in heat transfer with the Reynolds number as the solids mass fraction increases.

The heat transfer correlations presented in this section divide the flow in a laminar and a turbulent flow regime with a transition region in-between. However, the laminar regime can be further divided into a pure laminar and a wavy laminar regime. Al-Sibai [13] has carried out a comprehensive study of flow characteristics for falling film evaporation using a set of silicon oils with significant viscosity differences and, among others, developed correlations for the transition between pure laminar, wavy laminar and turbulent as a function of the Kapitza number. The heat transfer will also be dependent on whether evaporation or boiling is occurring, which is determined by the heat flux. This has been studied by for example Pavlenko [14], but in the work presented here, as the heat fluxes were low, only evaporation was occurring.

2.1. Simplified model

Johansson et al. [15] also developed a simplified implementation-oriented model for black liquor where the heat transfer coefficient is a function of specific mass flow rate and viscosity:

$$h = 201\Gamma^{0.26}\mu^{-0.41}. \quad (18)$$

This correlation was mainly developed for the turbulent region and is valid for $0.3 < \Gamma < 1.1$ kg/ms and $0.001 < \mu < 0.024$ Pas. The correlation showed good agreement with their experimental data and the variations in heat transfer were accurately described using only the specific mass flow rate and viscosity. Even though this model is limited to only softwood black liquor, does not account for flow regime and only consider two physical parameters, it could be valuable while simulating and designing industrial black liquor evaporators.

3. Experimental

A pilot falling film evaporator was used in this work and a schematic of the experimental set-up is seen in Fig. 1. The pilot evaporator was designed to be large enough to produce results relevant to industrial conditions, but also small enough so that a barrel of black liquor would be sufficient to run it. The heat transfer surface of the evaporator was a vertical tube, 60 mm outer diameter and 4.5 m long, giving an active outer heat transfer area of 0.848 m², with the falling liquid film on the outside. As in industry, the black liquor was heated with condensing saturated steam, in this case on the inside of the tube. The heating steam was distributed along the inside of the evaporator tube through an internal steam tube. The incoming steam was bubbled through a vessel containing condensate to ensure saturated conditions. The black liquor was fed to the top of the evaporator using a circulation pump, and partially evaporates while flowing down along the tube. In order to obtain a circumferentially uniform liquor distribution for a variety of flow rates, an overflow distributor integrated to the tube top was used. To minimize the effects of sputtering, a sputtering feedback device was used to collect the sputters and return them to the film.

The produced black liquor vapor was separated from the liquid fraction in a flash tank. The bottom of the flash tank was connected to the circulation pump. The vapor was sucked to a condenser which controlled the pressure. The produced condensate could

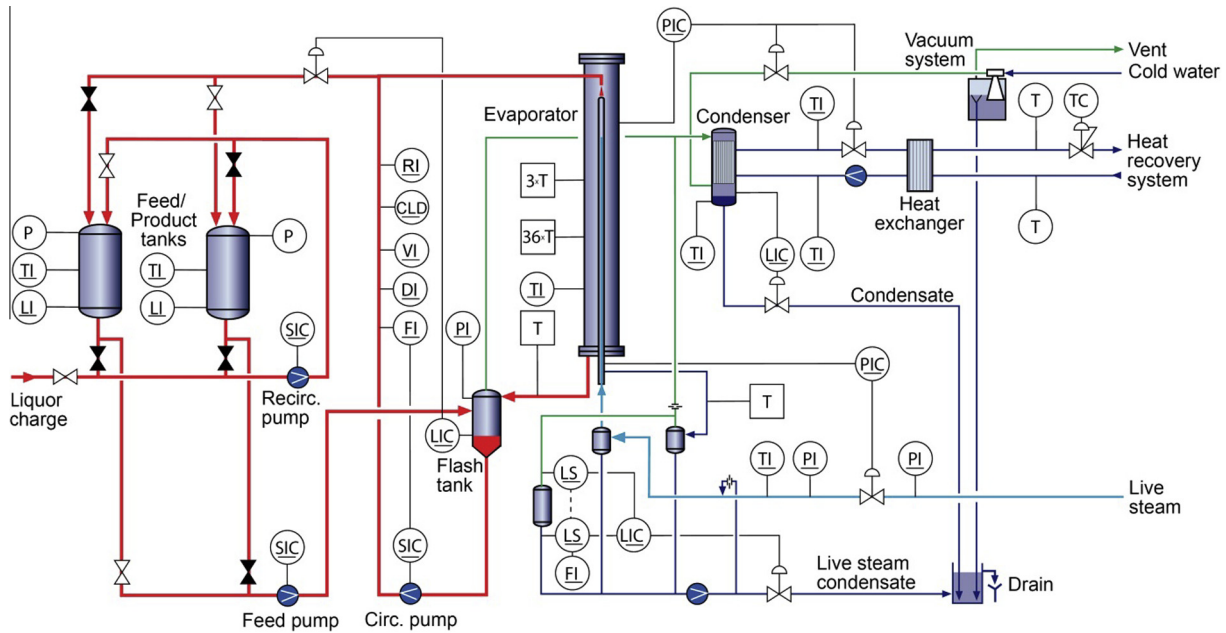


Fig. 1. Flow sheet of the research evaporator.

either be removed and collected outside the evaporator, or it could be recirculated to the flash tank to keep the dry solids mass fraction constant.

The pilot evaporator is highly instrumented with sensors to monitor the operation and to collect data. The most important measurements for this study were:

- Temperatures at multiple positions in the system.
- Pressure on both the heating steam side and the black liquor side of the evaporator.
- The mass flow rate and density of the circulating black liquor (Endress & Hauser Coriolis mass flow meter).
- The viscosity of the circulating black liquor (Marimex, Visco-scope- Sensor VA-300L).

More detailed description is given in e.g. [10].

3.1. Heat transfer measurements

The total heat transfer coefficient, i.e., the average of the entire heat transfer surface, is based on the measurement of the steam condensate flow, which is a direct measurement of the rate of heating, Q_{tot} . To obtain a condensate flow value solely related to the heating of the tube, background losses have been measured separately and were subtracted. From the rate of heating, the overall heat transfer coefficient, U , related to the outer area, A_o , was calculated as:

$$U = \frac{Q_{\text{tot}}}{A_o(T_{\text{steam}} - T_{bl})} \quad (19)$$

The steam temperature, T_{steam} , has been determined from the pressure and the liquor temperature, T_{bl} , from a “mixing cup” in the out-flow. From the overall heat transfer coefficient, the outer heat transfer coefficient, h_o , was calculated using the following expression:

$$\frac{1}{UA_o} = \frac{1}{h_i A_i} + \frac{\delta_w}{k_w A_m} + \frac{1}{h_o A_o}, \quad (20)$$

where δ_w is the thickness of the evaporator tube, i.e., 5 mm, k_w is the conductivity of the steel and A_m is the logarithmic mean area:

$$A_m = \frac{A_o - A_i}{\ln\left(\frac{A_o}{A_i}\right)} \quad (21)$$

The inner heat transfer coefficient, h_i , has been estimated using a correlation for condensation on vertical surfaces by Schnabel and Palen [16]. Since the black liquor was flowing on the outside of the tube, the outer heat transfer coefficient was the one of interest and could be calculated using Eq. (20) since all other variables were known.

It was also possible to measure local heat transfer at 6 different vertical and circumferential positions along the tube using pairs of thermocouples that were soldered into the tube wall. For this work, they were, however, only used to verify the total heat transfer measurements and to detect fouling. For more details concerning the local heat transfer measurements, see Johansson et al. [2].

3.2. Physical properties of the fluid

Viscosity is very important for heat transfer analysis of falling films. The process viscometer measured the viscosity of the liquid continuously inline using the torsional oscillation principle [17]. The viscometer measured viscosity at an almost constant shear rate of 3450 s^{-1} , which was significantly higher, at least for lower Reynolds numbers, than the shear rates in the falling film. Black liquor can behave as either a Newtonian or a non-Newtonian fluid and this behaviour can change with the dry solids mass fraction and temperature. Since the composition of the liquor changes depending on its origin, different conclusions are found in the literature for when it could be considered Newtonian. However, when there is a non-Newtonian behaviour (shear thinning) it is stronger at high dry solids mass fraction and low temperature [1].

Softwood (which was used in this study) is normally more Newtonian than hardwood and, among all, Söderhjelm [18], Moosavifar et al. [19] and Wennberg [20] concluded that softwood black liquor could be seen as a Newtonian fluid. This is especially true at the high temperatures used in industrial evaporators which was shown by Sandquist [21] and Zaman and Fricke [22]. However, a small investigation of rheology was included in Johansson et al. [10] and here a shear rate dependency was found for a softwood

liquor at temperatures used in the industry. Other studies concluding that black liquor is non-Newtonian were normally performed at temperatures lower than what is used industrially or used samples originating from hardwood. For example, Tiu et al. [23] measured a shear-rate dependence of a black liquor in the dry solids mass fraction range of 0.47–0.75, but this was for liquor originating from eucalyptus which is a type of hardwood with strong non-Newtonian behaviour. Since the majority of the studies conclude that softwood liquors is Newtonian and since the study by Johansson et al. [10] is rather limited in terms of samples and measurements, Newtonian behaviour is assumed in this study, especially since high temperatures were used (further described in section 3.3).

The conductivity and heat capacity of the black liquor needed for the dimensionless number analysis were calculated with correlations given by Adams et al. [1]. The dry solids mass fraction of the black liquor was measured from samples that were taken out of the evaporator, using TAPPI test method T650 om-89.

As water evaporates from the falling film, the black liquor properties will be slightly different at the top and bottom of the tub. It was, however, assumed that the flow rate was high enough to neglect this difference. This assumption is validated and discussed in Section 4.4.1. All important parameters (i.e., dry solids mass fraction, viscosity, mass flow rate and density) were therefore measured for the incoming liquor, except for the mixing cup temperature and boiling point elevation which were measured in the outflow.

3.3. Experimental method and conditions

In this study, the heat transfer coefficient at different black liquor dry solids mass fractions, between 0.45 and 0.85, were investigated while also varying temperature and flow rate. The temperatures used were similar to those used in the industry, i.e., 100 °C for the lower dry solids mass fraction and up to 175 °C for the highest mass fraction. For the majority of the measurement points, a low and a high specific mass flow rate of $\Gamma = 0.9$ and $\Gamma = 2$ kg/ms were used. These limits were chosen to avoid dry out at the low flow and sputter at the high flow, but still to give a significant difference. See Table 1 for details about the operational conditions.

All experimental results presented in this paper are from the same black liquor originating from a Swedish kraft pulp mill using softwood. Prior to the actual experiments, all of the black liquor

was pre-evaporated at 100 °C to the desired feed dry solids mass fraction of 0.45.

To reach the desired conditions for the different measurements, the liquor was first heated to the desired temperature without evaporation. Thereafter, the evaporator was operated in semi-batch mode where the black liquor vapor produced was removed to increase the concentration. Once all desired conditions were reached, the mode of operation was switched to continuous, meaning that the vapor was still removed but now fresh low concentrated black liquor was fed to the system, while the more concentrated product liquor was ejected to keep the system volume constant. For the highest dry solids mass fraction (0.85), the heat transfer was too low to heat the entering liquor and therefore batch operation was used, i.e., no in- or outflow of liquor, and the condensed vapor was mixed back with the liquid.

The continuous operation was chosen to minimize the residence time and thereby thermal treatment of the black liquor. Thermal treatment occurs when black liquor is kept at an elevated temperature and is the effect of residual alkali in the black liquor breaking down polysaccharides and lignin to lower molecular weight compounds which decreases the viscosity [24,25]. However, this process will also decrease the residual alkali level and pH, and then, if the level gets too low, the shape of the lignin molecules expand and associate to form large complex molecules, leading to a decrease of the apparent molecular weight and increase of the viscosity [1]. As long as the residual alkali level is above 0.03 kg Na₂O/kg dry solids there should be no such effect on the viscosity according to Milanova and Dorris [26]. Both of these counteractive effects are reduced as the average residence time is reduced.

3.3.1. New method to overcome fouling

Fouling of the heat transfer surface can cause a significant decrease in heat transfer. For black liquor, fouling is common for a dry solids mass fraction above about 0.5 since then sodium salts starts to crystallize. This makes it difficult to measure the true heat transfer coefficient at higher dry solids mass fractions since clean conditions are needed. When running experiments it takes time before the desired conditions are reached and fouling might influence the measurements.

To avoid fouling influencing the heat transfer measurements, a special method had to be developed. Thus, prior to a measurement, the heat transfer surface was cleaned without shutting-down the evaporator system as a whole. The liquor, which is normally fed to the top of the evaporator, was instead recirculated directly to

Table 1
Operation conditions and fundamental results.

Dry solids (kg/kg)	Density (kg/m ³)	Liquor temperature (°C)	Heat flux (W/m ²)	Mass flow rate (kg/m s)	Dynamic viscosity (Pa s)	Heat transfer coefficient (W/m ² K)
0.436	1220	110	11100	0.89	0.0017	2190
0.440	1228	100	10200	0.90	0.0022	1880
0.440	1228	100	10400	2.00	0.0022	1970
0.559	1280	110	9300	0.52	0.0073	1450
0.559	1280	110	9500	2.04	0.0073	1600
0.615	1300	130	8400	0.91	0.016	1300
0.615	1300	130	8700	2.00	0.012	1550
0.615	1320	110	8900	2.02	0.012	1500
0.667	1340	140	8300	2.00	0.017	1400
0.671	1350	130	8400	0.91	0.028	1300
0.671	1350	130	8200	2.00	0.028	1350
0.726	1370	160	7400	2.00	0.028	1100
0.724	1390	140	6700	0.91	0.067	900
0.724	1380	140	7800	2.00	0.067	1150
0.786	1420	160	4800	2.10	0.16	600
0.849	1460	175	3500	1.50	0.57	140

the flash tank to maintain mixing of the liquor and thereby avoid possible sedimentation or solidification. Water was then fed to the top of the evaporator tube through the ordinary liquor distributor and was allowed to rinse the tube as long as there was visible fouling. Since the fouling mainly consisted of sodium salts that were easily dissolved in the method was efficient. Once the surface was considered clean, the washing operation was terminated and the normal operation was switched back and the measurement could start. The cleaning should, however, be done as quickly as possible to avoid unnecessary cooling of the liquor. For dry solids mass fractions above 0.75, the risk was considered too high for performing the cleaning sequence. If the flow of black liquor stops at these concentrations it would cool fast and become too viscous for further operation, causing a plant shut down.

4. Results and discussion

4.1. Experimental results

The main experimental data are presented in Table 1. The results consist of seven different levels of dry solids mass fractions, and for four of these levels, two different temperatures and specific mass flow rates. At a dry solids mass fraction of 0.559, a significantly lower specific mass flow rate was tested, $\Gamma = 0.5$ kg/ms, compared to the rest of the experiments. For the two highest liquor concentrations, only one specific mass flow rate and one temperature were tested. Since the experiment at the highest concentration had very poor heat transfer, a higher temperature difference between liquor and heating steam was used; i.e., 25 °C instead of 10 °C as for the other experiments.

In general, only minor fouling could be observed visually while cleaning the tube or from the trends in total and local heat transfer coefficients. However, in the cases where fouling was building up during the measurements, the trends of the heat transfer coefficients could be analyzed to estimate the value for clean conditions since the tube was cleaned just before the measurement started. For the experiments at 0.79 and 0.85 dry solids mass fractions, no cleaning could be performed, but from visual observations and by analyzing the trend in total and local heat transfer coefficient, no evidence of fouling was found.

Residual alkali was measured initially and for two experiments. The initial residual alkali level was 0.027 kg Na₂O/kg dry solids and at $S = 0.559$ it was 0.024 kg Na₂O/kg dry solids, meaning that the measurement points at lower dry solids mass fractions only showed limited effects of heat treatment. At $S = 0.849$ the residual alkali was 0.017 kg Na₂O/kg dry solids. However, it was probably mainly the point at the highest dry solids mass fraction that was affected since then continuous operation was not possible. The residual alkali level was generally low compare to the limit mentioned by Milanova and Dorris [26] (0.03 kg Na₂O/kg dry solids), meaning that the viscosity was probably higher than what would have been observed at a higher alkali level.

It should be noted that the hydrodynamics of the falling film in these experiments became increasingly chaotic along the tube and far from a film of uniform thickness and distribution in the lowest part of evaporator, especially at the highest viscosities or Prandtl numbers. This can be seen in Fig. 2, which shows the typical behavior of the film in the top and bottom of the evaporator. In the top, the film had uniform thickness and distribution except for some waves, but due to wave brake down, bubbles and sputters, the film was uneven in the bottom. Bubbles are not formed due to nucleate boiling, rather other mechanisms are causing the bubble formation, which was discussed in detail in Johansson et al. [27]. In all experiments, except for the point with the highest viscosity, no dry out was observed and even though the flow was uneven in

the bottom the flow only disappeared locally for maximum about one second and then came back again. The sputtering feedback device was able to return most of the sputtered liquor back to the tube. Even though the viscosity was very different in the different experiments, the hydrodynamics behavior was similar and did not deviated much from Fig. 2. No foam was formed.

In Fig. 3, the heat transfer coefficients obtained are shown versus viscosity. Due to fluctuations in the measurements there are some uncertainties in the values of the heat transfer coefficient, which are indicated by error bars. The maximum and minimum values give the span which should include the true value and this was set by analyzing the amplitude and trend of the fluctuations.

From Fig. 3 it is difficult to see the dependence on specific mass flow rate. In Fig. 4, pairs of measurement points at the same viscosity (i.e., the same dry mass fraction and temperature) but at high and low specific mass flow rates are presented.

4.2. Comparison with simplified correlation

As seen in Figs. 3 and 4, the heat transfer coefficient is influenced by both specific mass flow rate and viscosity. However, the dependence on specific mass flow rate is relatively weak while the dependence on viscosity is strong and explains most of the variations in the data. To further analyze these relations, Γ and μ have been fitted to a correlation of the same form as Eq. (18):

$$h = K\Gamma^{P_\Gamma}\mu^{P_\mu} \quad (22)$$

using K , P_Γ and P_μ as adjustable parameters. The result of the fit is presented in Table 2.

This simplified type of correlation do not consider whether it is laminar or turbulent flow and the heat transfer coefficient is modeled using only the specific mass flow rate and dynamic viscosity. Other physical properties, such as heat capacity and conductivity, also affect the heat transfer coefficient, but do not change as radically as the viscosity. Since all physical properties of interest will vary with temperature and dry solids fraction, they will all be incorporated into the parameter of the viscosity. This means that P_μ does not represent the true viscosity dependence but rather it represents a change in all physical properties.

When analyzing the data, the point with the highest viscosity ($\mu = 0.57$ Pas) shows a deviation from the trend of the rest of the points. Due to reasons mentioned below, there were some uncertainties in the measurements at this point and, therefore, the curve fitting was performed both with and without this point. When the point was excluding, the R^2 value increased from 0.89 to 0.92 and the confidence interval decreased for both P_Γ and P_μ , meaning better agreement with the data.

In Fig. 5, the correlation without the point for the highest viscosity has been plotted together with the correlation by Johansson et al. [15]. In Fig. 5, the heat transfer coefficient is displayed with a logarithmic scale, and this shows more noticeably than in Fig. 3 that the highest point deviates. The correlation by Johansson et al. [15], which was validated for black liquor at lower viscosity and specific mass flow rate than used here, showed a higher dependence of specific mass flow rate and viscosity than the data in this work. There can be at least two reasons for this; either the higher dry solids mass fraction and viscosity give substantial changes in fluid properties, or else the experiments in this study were operating in a higher range of specific mass flow rate ($\Gamma = 0.5$ – 2 compared to $\Gamma = 0.3$ – 1.1). However, the data in this work is limited in terms of specific mass flow rate and more experiments are needed to draw any comprehensive conclusions. Since the 95% confidence interval of P_Γ does not exclude zero or negative value (lower limit – 0.037) it is not statistically significant that

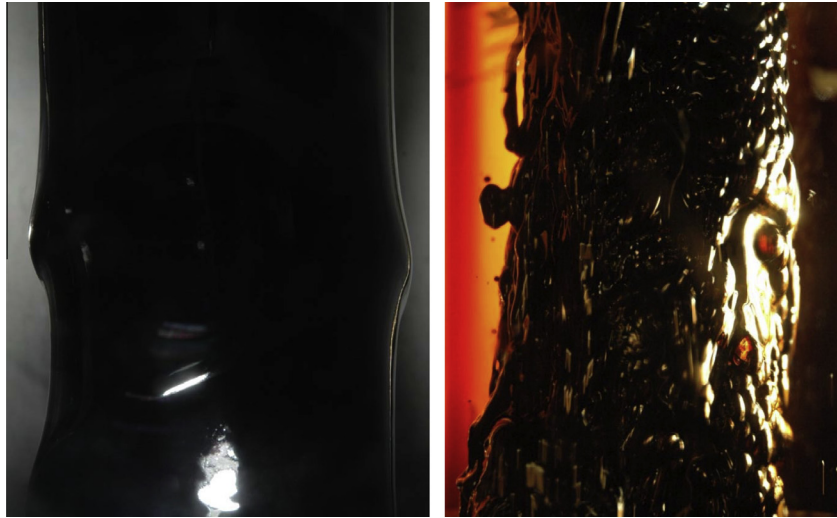


Fig. 2. Hydrodynamic behavior of the falling film at $q = 7700$, $Re = 230$ and $Pr = 209$ (left) at the top (0.3 m from inlet) of the evaporator tube and (right) at the bottom (4 m from inlet).

there actually is a dependence on the specific mass flow rate in the investigated region.

The dependence on viscosity for the data in this work is indicated by an exponent of -0.21 compared to -0.41 for Johansson et al. [15]. Their model does not follow the general trend of the experimental data which is clear from Fig. 5. This means that the heat transfer for black liquor cannot be easily described for the whole range of viscosities by this type of simplified model without changing the parameter values.

4.3. Comparison with general correlations

The general correlations for heat transfer explicitly include heat capacity, thermal conductivity and density, whereas for the simplified correlation presented above, these fluid properties' influence are mainly incorporated into the viscosity parameter. The general correlations also account for the flow regime, where the Nusselt number normally decreases with increasing Reynolds number in the laminar region and, vice versa in the turbulent region.

In Fig. 6, the experimental Nusselt numbers are presented as a function of the Reynolds number at different Prandtl numbers. Points with the same Prandtl numbers are connected with lines. The reader should keep in mind that all three of these dimensionless numbers are a function of viscosity which by far is the most dominant variable. For the Nusselt number, which measures the relative importance of convection heat transfer compared to conduction, it is expected that high Nusselt numbers imply high heat transfer. Here, in contrast, the increase at elevating dry solids mass fractions is driven by viscosity, but the heat transfer actually decreases. From Fig. 6 it is clear that the point with the highest Prandtl number ($Pr = 2804$) deviates from the trend of the other points. The Nusselt number increases with an increase in Reynolds number for constant Prandtl numbers, and this indicate that at least the points with the higher flow are turbulent. The flow is probably close to the transition region between laminar and turbulent flow and the scarcity of measurements makes it difficult to draw any conclusions with certainty.

The transition from laminar to turbulent flow is not only dependent on the Reynolds number but also the Prandtl or Kapitza num-

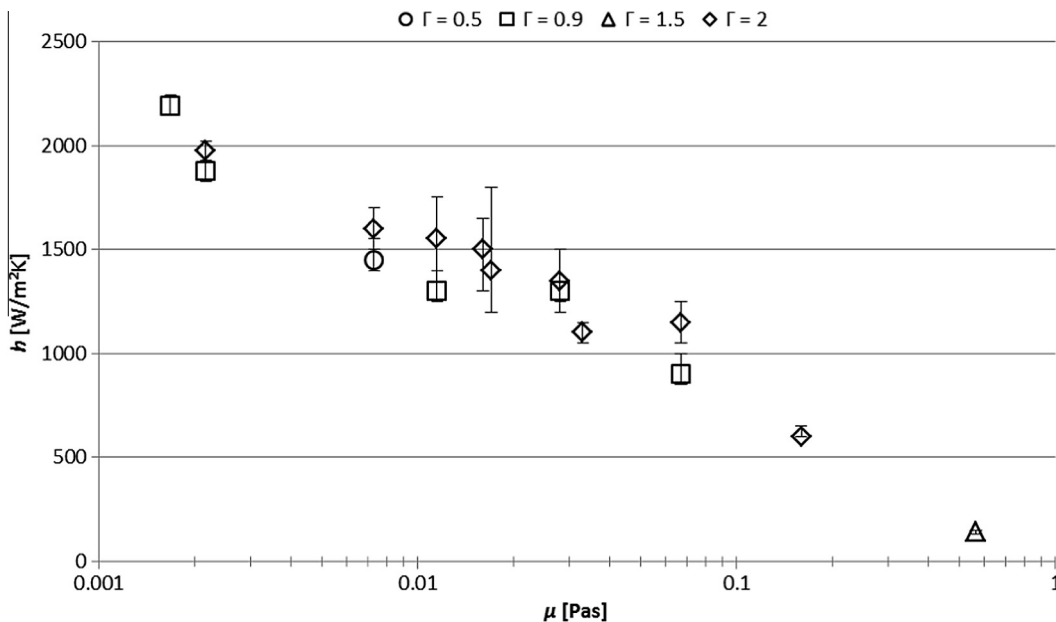


Fig. 3. Heat transfer coefficient as a function of dynamic viscosity for different specific mass flow rates, error bars show uncertainties due to fluctuations in measurements.

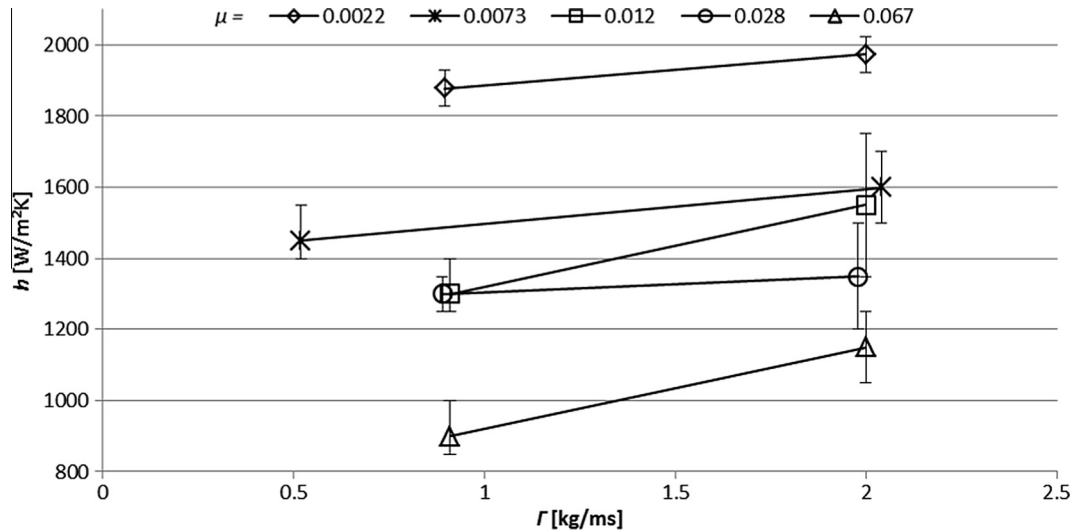


Fig. 4. Heat transfer coefficient at high and low specific mass flow rates for black liquor at 5 different viscosities, error bars show uncertainties due to fluctuations in measurements.

Table 2
Parameters in simplified correlations for this work and Johansson et al. [15].

	K	P_r	P_μ	Correlation P_r and P_μ	R^2
This work, all points	489	0.089 ± 0.16	-0.23 ± 0.06	-0.30	0.89
This work, $\mu = 0.57$ excluded	558	0.073 ± 0.11	-0.21 ± 0.04	-0.31	0.92
Johansson et al. [15]	201	0.26 ± 0.12	-0.41 ± 0.05		

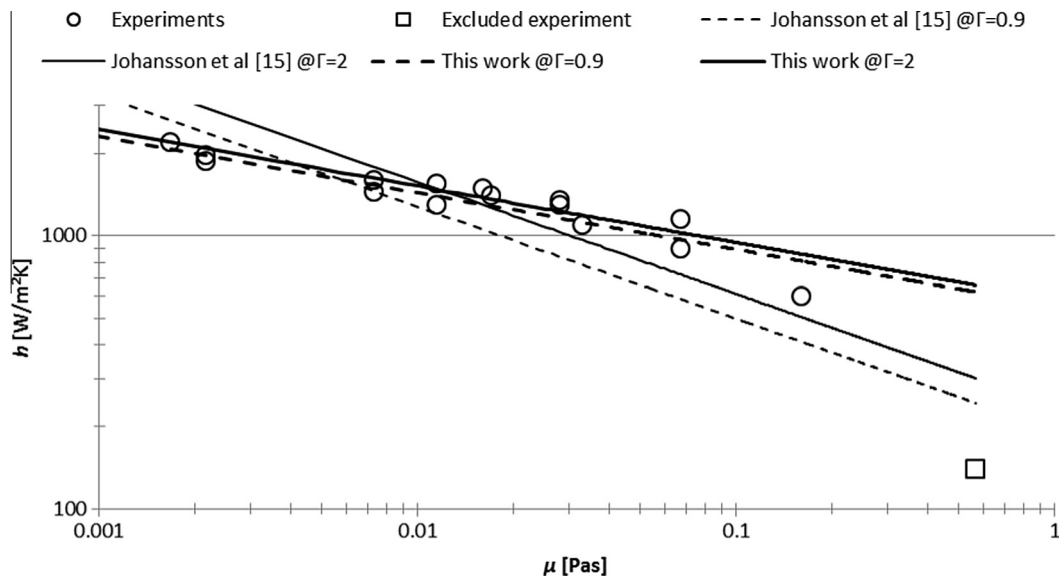


Fig. 5. Experimental heat transfer coefficient as a function of viscosity together with simplified correlations.

ber. If the expression by Chun and Seban [9], Eq. (3), is extrapolated to the high Prandtl numbers used here, it suggests that all the experimental points are in the turbulent region. However, the study by Al-Sibai [13], where the transition is described in more detail for fluids with relatively high viscosity, predicts that the majority of the points are in the transition between wavy-laminar and turbulent but with a few exceptions; the highest Reynolds number is turbulent, and a few points are wavy-laminar. The visual observations indicate that the flow was a combination of wavy-laminar and turbulent, but, again, it was hard to classify the measurements into a specific flow regime.

In Figs. 7 and 8 the experimental Nusselt number is compared with predictions from the general correlations by Schnabel and Schlünder [8], Chun and Seban [9], Arndt and Scholl [11] and Johansson et al. [2]. It is important to emphasize that none of these general correlations have actually been validated for these high Prandtl numbers.

For the lowest Prandtl numbers (or highest Reynolds numbers), Johansson et al. [2] show the best agreement with the experimental data. This is reasonable since this correlation has been specially adapted to black liquor and validated for the conditions at these points. Schnabel and Schlünder [8] and Chun and Seban [9] have

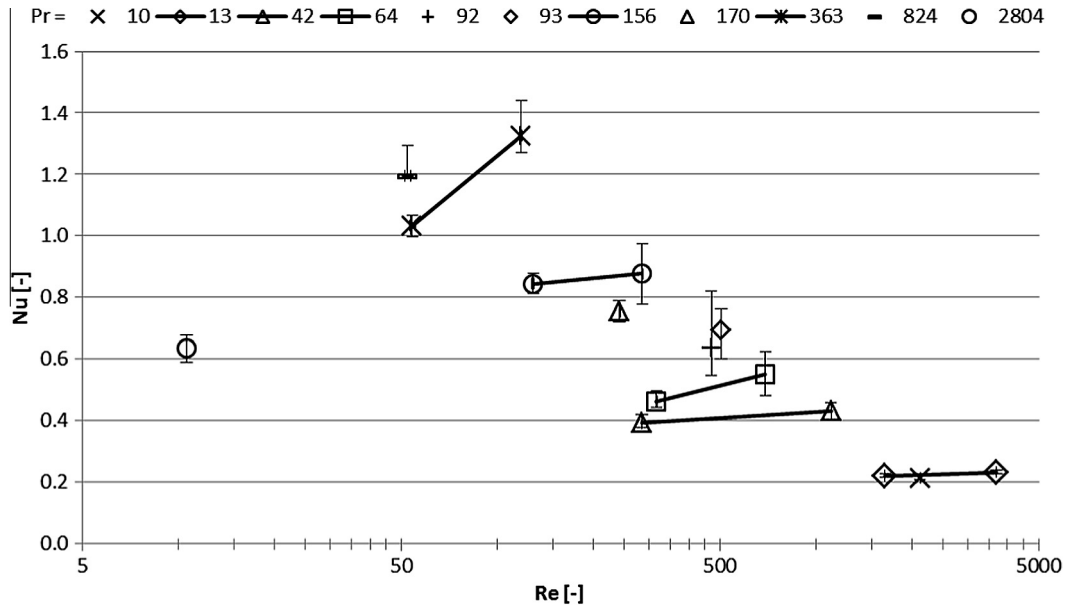


Fig. 6. Nusselt number for the experimental data as a function of Reynolds number, where the points at the same Prandtl numbers are connected with lines.

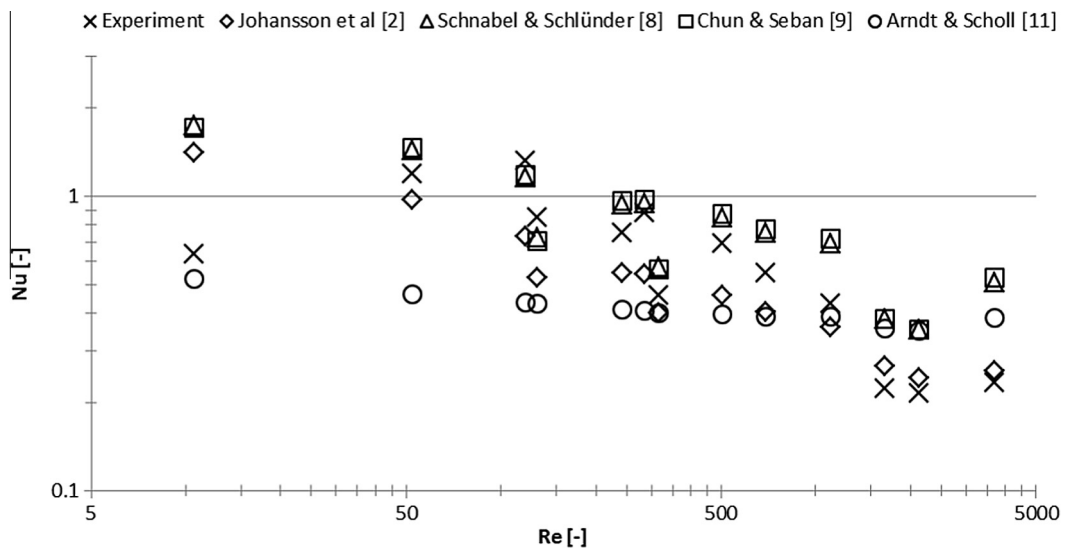


Fig. 7. Nusselt number for the experimental data as a function of the Reynolds number compared with correlations. Some overlapping data points were excluded to make the figure clearer.

the worst predictions at these low Prandtl numbers with a Nusselt number that is too high, but as the Prandtl number increases their predictions are the best. This is in line with the work by Johansson et al. [10], who also found that Schnabel and Schlünder [8] and Chun and Seban [9] over-predicted the heat transfer for black liquor at lower Prandtl numbers but showed good agreement above $Pr = 52$. The two correlations are very similar, except that the predictions from Schnabel and Schlünder [8] are somewhat lower, thus giving these predictions a slightly better agreement with the experimental data. The correlation by Johansson et al. [2] predicts a Nusselt number that is too low for the higher Prandtl numbers. Except for the lowest Prandtl numbers, Arndt and Scholl [11] predict an even lower Nusselt number than Johansson et al. [2] and they do not really follow the trend of the data here. One reason could be that their correlation predicts the data to be closer to the laminar region while the other correlations predict it to be mainly in the turbulent region. The points at the highest Reynolds numbers, which were predicted turbulent or close to turbulent by

Al-Sibai's characterization [13], were clearly laminar according to Arndt and Scholl [11].

To quantify how well the different correlations predicted the experimental data, the R^2 -value could be used. Note that some points were removed to make Figs. 7 and 8 more visible, but when the R^2 -values were calculated all points but the one at the highest Prandtl number were included. Schnabel and Schlünder [8] had the best prediction, $R^2 = 0.73$, closely followed by Chun and Seban [9] at $R^2 = 0.69$. The predictions from Johansson et al. [2] were less good, $R^2 = 0.47$, and Arndt and Scholl's [11] predictions were the least accurate, $R^2 = -0.47$. The negative value should be interpreted as the predictions are worse than using a constant value for all points, i.e., the model did not follow the trend of the data. Consequently, the R^2 -analysis gave the same results as indicated by Figs. 7 and 8.

Fig. 9 presents more clearly how well the experimental data are predicted by Schnabel and Schlünder [8]. Again, it is shown that the agreement is good at the higher Prandtl numbers, except for

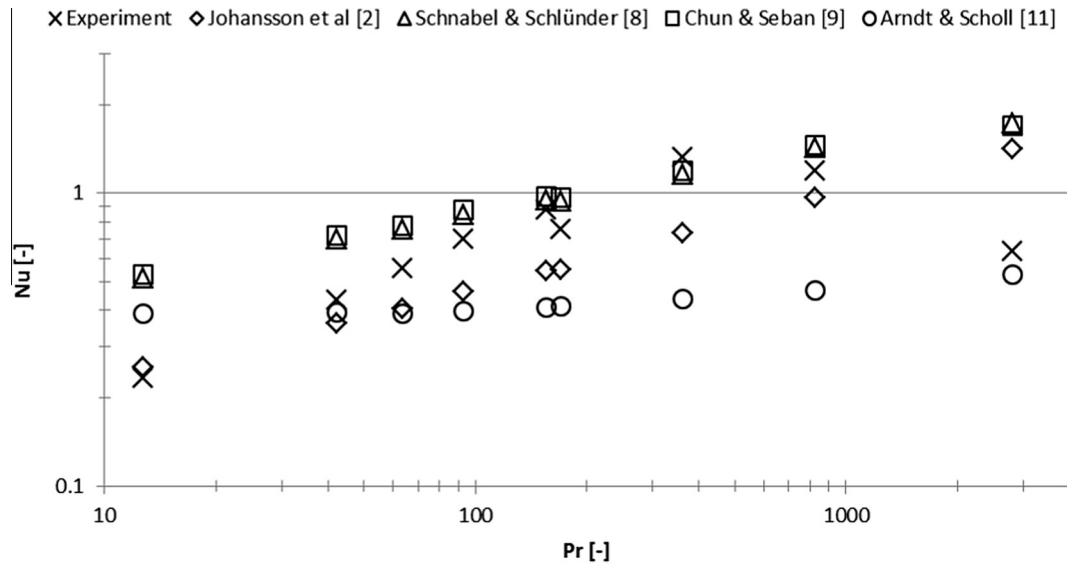


Fig. 8. Nusselt number for the experimental data as a function of the Prandtl number compared with correlations. Some overlapping data points were excluded to make the figure clearer.

the point at $Pr = 2804$. $Pr = 10$ and 13 are less good. According to this extrapolation of Schnabel and Schlünder [8], the experimental point are in the turbulent region, but close to the transition region between laminar and turbulent. Due to low variation of the Reynolds number it is not possible to say if it is the Prandtl number dependence or the model for the transition region that should be adjusted to get a better fit with experimental data. As mentioned above, correlation by Al-Sibai [13] gives a slightly different picture regarding the flow regime.

When summarizing all the analyzed models, neither the simplified nor the available general correlations seem to be able to describe the whole span of dry solids mass fractions for black liquor using the same parameters. This indicates that there is a change in the physical or hydrodynamic behavior of the liquor that

is not covered by the models and that further research is needed to develop a complete model.

4.4. Uncertainty analysis

4.4.1. Property variations along the tube wall

The properties of the liquor have been considered constant along the tube, even though this is actually not true. Especially data for low specific mass flow rates is sensitive to this assumption. Therefore the effect of the mass fraction increase along the tube for two of the most important parameters; the boiling point elevation and viscosity, are estimated in Table 4 using correlations from Adams et al. [1]. Knowing the increase in viscosity, the effect on the heat transfer measurements has been estimated using Eq. (22). As mentioned previously,

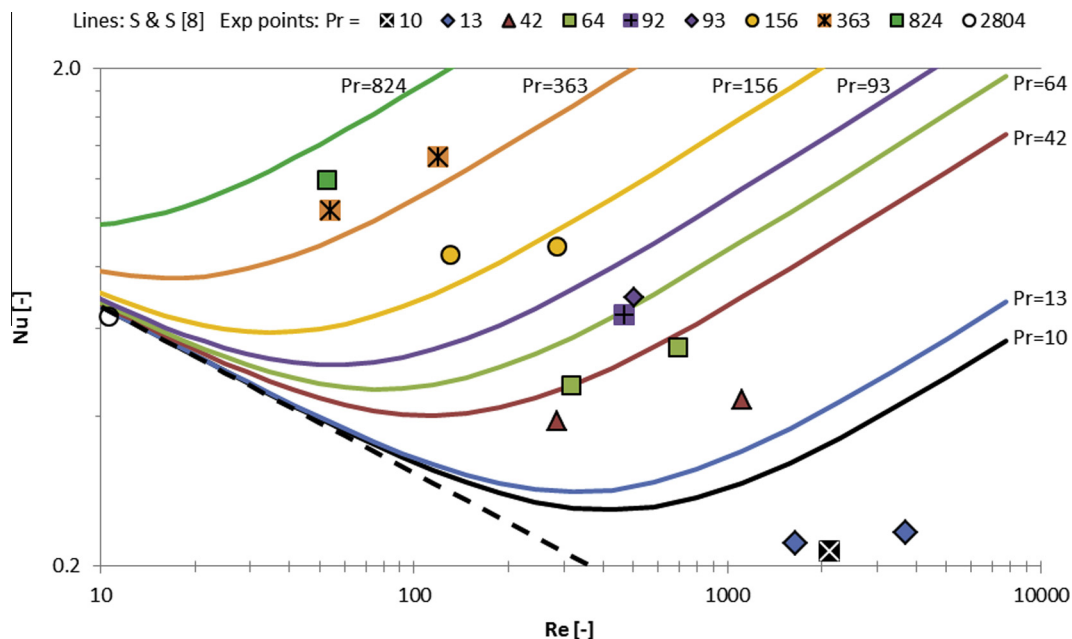


Fig. 9. Comparison of experimental data and correlation from Schnabel and Schlünder [8]. The dashed line is the laminar correlation. The solid lines represent the prediction corresponding to the experimental data having the same color.

Table 3

Estimation of the increase in dry solids mass fraction, viscosity and boiling point elevation from the inflow to the outflow of the tube and their consequential effect on the local heat transfer coefficient.

Estimated change in liquor property along the tube	$\Gamma = 0.5$	$\Gamma = 0.9$	$\Gamma = 2$
Dry solids mass fraction	+0.017	+0.012–0.013	+0.004–0.006
Boiling point elevation	+0.7 °C	+0.6–0.9 °C	+0.2–0.5 °C
Dynamic viscosity	+25%	+17–22%	+6–9%
Estimated effect on the heat transfer coefficient	–5%	–4–5%	–1–3%

all the properties of the black liquor, except for the temperature, were measured at the inflow to the tube.

The estimated increase along the tube in boiling point elevation is 0.9°C, meaning that the boiling point temperature and surface temperature are not exactly constant along the tube which has been assumed. The effect on viscosity is relatively high; a 25% difference between the inlet and outlet for the lowest specific mass flow rate. However, the maximum effect on the heat transfer has been estimated to be only 5%. Even though the heat transfer measurements at lower specific mass flow rates are more affected by the property changes along the tube, this effect is limited and cannot explain the differences that have been measured between high and low specific mass flow rates (Fig. 4). When comparing the properties at the inflow with the average, all figures in Table 3 should be halved (if using an arithmetic average), making the error when neglecting the change along the tube reasonably low.

4.4.2. Hydrodynamics of the falling film

The hydrodynamics of the falling film under the conditions investigated are increasingly chaotic in the direction of the flow and the liquid film will not maintain a uniform thickness and distribution, as described in Section 4.1. In the current experimental setup efforts were taken to have a uniform distribution in the top and minimize the effect of sputtering. In terms of modeling better understanding is needed when developing more comprehensive models, but this was not further investigated in this study.

4.4.3. Viscosity measurements

As previously concluded, viscosity is the most important parameter in this study and therefore accurate measurements are important. There are some uncertainties whether the black liquor used in this study could be treated as a Newtonian fluid. However, since most of the literature reports that softwood black liquor is Newtonian it should be reasonable to assume here as well.

5. Conclusions

- A new method to overcome problems with fouling under crystallizing conditions has been successfully developed and enables reliable measurements of heat transfer for black liquor evaporation at dry solids mass fractions up to at least 0.75.
- In the high-to-very high Prandtl number region, viscosity is by far the most dominant parameter for the heat transfer for the investigated conditions.
- For the measured conditions the heat transfer increased at higher specific mass flow rates, but the dependence was weak and not statistically significant.
- Available correlations for heat transfer and flow characterization gave partly different results when predicted the flow regime.
- Despite that the correlations by Schnabel and Schlünder [8] have been extrapolated extremely far from the original validity, the agreement with the experimental data was reasonable good for Prandtl numbers from 90 to 800. However, below 90 the correlation overestimates the heat transfer. The correlations by Chun and Seban [9] showed similar results.

- The more recently developed correlations by Johansson et al. [2] and Arndt and Scholl [11] clearly underestimate the heat transfer, especially the later, at the high Prandtl numbers used in this study.
- None of the studied correlations have been able to capture the heat transfer behavior for black liquor throughout the whole range of Prandtl numbers. This should not be interpreted as weaknesses of the models since they were extrapolated very far from where they were validated, but rather that black liquor, and likely other fluids at very high Prandtl numbers as well, needs new models to comprehensively predict the heat transfer.
- To be able to accurately model the heat transfer of highly concentrated black liquor better understanding of the hydrodynamic is needed together with detailed measurements of its physical properties.

Acknowledgments

This work was co-funded by the Swedish Energy Agency, Metso Power AB, Troëdssons forskningsfond and Chalmers Energy Initiative.

References

- [1] T.N. Adams, W.J. Frederick, T.M. Grace, M. Hupa, K. Iisa, A.K. Jones, H. Tran, Kraft Recovery Boilers (1997).
- [2] M. Johansson, L. Vamling, L. Olausson, Heat transfer in evaporating black liquor falling film, *Int. J. Heat Mass Transfer* 52 (11–12) (2009) 2759–2768.
- [3] H. Mueller-Steinhagen, C.A. Branch, Heat transfer and heat transfer fouling in Kraft black liquor evaporators, *Exp. Therm. Fluid Sci.* 14 (4) (1997) 425–437.
- [4] C.A. Branch, H. Müller-Steinhagen, Convective and subcooled flow boiling heat transfer to kraft black liquor, *Appita* 44 (2) (1993) 114–118.
- [5] V.A. Suslov, Y.N. Zayatz, Increase in sulfate black liquor recovery efficiency: Evaporator performance, in: Proceedings of 2007 International Chemical Recovery Conference – Efficiency and Energy Management, Quebec City, QC, Canada, May 29–June 1, 2007 (2007).
- [6] F.C. Chen, Z. Gao, An analysis of black liquor falling film evaporation, *Int. J. Heat Mass Transfer* 47 (8–9) (2004) 1657–1671.
- [7] E.O. Doro, Computational modeling of falling liquid film free surface evaporation, Dissertation, Georgia Institute of Technology, 2012.
- [8] G. Schnabel, E.U. Schlünder, Wärmeübergang von senkrechten Wänden an nicht-siedende und siedende Rieselfilme. "Heat Transfer from Vertical Walls to Falling Liquid Films with or Without Evaporation", *Verfahrenstechnik* 14 (2) (1980) 79–83.
- [9] K.R. Chun, R.A. Seban, Heat transfer to evaporating liquid films, *J. Heat Transfer, Trans. ASME* (1971) 391–397.
- [10] M. Johansson, L. Vamling, L. Olausson, Falling film evaporation of black liquor – Comparison with general heat transfer correlations, *Nordic Pulp Paper Res. J.* 21 (4) (2006) 496–506.
- [11] S. Arndt, S. Scholl, Evaporation of single component viscous liquids in a metal falling film evaporator, *Heat Mass Transfer/Waerme Stoffuebertr* 47 (8) (2011) 963–971.
- [12] A.A. Alhousseini, K. Tuzla, J.C. Chen, Falling film evaporation of single component liquids, *Int. J. Heat Mass Transfer* 41 (12) (1998) 1623–1632.
- [13] F. Al-Sibai, Experimentelle Untersuchung der Strömungscharakteristik und des Wärmeübergangs bei welligen Rieselfilmen, RWTH Aachen, Aachen, 2005.
- [14] A.N. Pavlenko, Hydrodynamics and heat transfer in boiling and evaporation in cryogenic falling films and applications, in: S. Kakaç, H.F. Smirnov, M.R. Avelino (Eds.), *Low Temperature and Cryogenic Refrigeration*, Springer, Netherlands, 2003, pp. 181–200.
- [15] M. Johansson, L. Vamling, L. Olausson, An implementation-oriented heat transfer model for black liquor evaporation, in: Proceedings of the

- International Chemical Recovery Conference 2007, May 29–June 1, 2007, Quebec City, Canada, 2007, pp. 155–158.
- [16] G. Schnabel, J.W. Palen, Wärmeübergang an senkrechten berieselten Flächen, VDI Wärmeatlas, eighth ed., Springer, Verlag, Berlin, 1998. Sect. Md.
- [17] <http://www.marimex.de/eng-technology-process-viscometer.php>, in, "MARIMEX Industries GmbH & Co".
- [18] L. Söderhjelm, Factors affecting the viscosity of strong black liquor, *Appita* 41 (5) (1988) 389–392.
- [19] A. Moosavifar, M. Sedin, H. Theliander, Changes in viscosity and boiling point elevation of black liquor when a fraction of lignin is removed – consequences in the evaporation stage, *Appita J.* 62 (5) (2009) 383.
- [20] O. Wennberg, Rheological properties of black liquor, in: International Chemical Recovery Conference, Ottawa, Canada, 1989, pp. 89–93.
- [21] K. Sandquist, Rheological properties and evaporation of black liquor at high solids content, Part I: Rheology, *Pulp Paper Canada* 84 (2) (1983) 31–34.
- [22] A.A. Zaman, A.L. Fricke, Viscosity of Black Liquor Up to 130 Degrees Celsius and 84% Solids, in: Forest Products Symposium, TAPPI PRESS, 1991.
- [23] C. Tiu, K.L. Nguyen, M. De Guzman, Non-Newtonian behaviour of kraft black liquors, *Appita* 46 (3) (1993) 203–206.
- [24] E. Vakkilainen, R. Backman, M. Forssten, M. Hupa, Effects of liquor heat treatment on black liquor combustion properties, *Pulp Paper Canada* 100 (8) (1999) 24–30.
- [25] J. Louhelainen, R. Alén, J. Zielinski, P.E. Sägfors, Effects of oxidative and non-oxidative thermal treatments on the viscosity and chemical composition of softwood kraft black liquor, *J. Pulp Paper Sci.* 28 (9) (2002) 285–291.
- [26] E. Milanova, G.M. Doris, Effect of residual alkali content on the viscosity of kraft black liquors, *J. Pulp Paper Sci.* 16 (3) (1990) 94–101.
- [27] M. Johansson, I. Leifer, L. Vamling, L. Olausson, Falling film hydrodynamics of black liquor under evaporative conditions, *Int. J. Heat Mass Transfer* 52 (11–12) (2009) 2769–2778.